Preprints of the 21st IFAC World Congress (Virtual)
Berlin, Germany, July 12-17, 2020

Scalable PI Voltage Stabilization in DC Microgrids

Mahdieh S. Sadabadi * **Qobad Shafiee** **

* *Department of Automatic Control and Systems Engineering, University of Sheffield, Sheffield, United Kingdom (e-mail: m.sadabadi@sheffield.ac.uk).*
** *Department of Electrical Engineering, University of Kurdistan, Sanandaj, Kurdistan, Iran (email: q.shafiee@uok.ac.ir).*

Abstract: This paper addresses the problem of decentralized PI-based voltage stabilization in islanded DC microgrids with DC-DC buck converters. We propose a voltage control approach with a decentralized PI control structure. The proposed voltage control design is scalable and does not rely on the global model of the microgrids and parameters of the distribution lines. Moreover, it guarantees the asymptotic stability of the DC microgrid systems. The scalability of the design and asymptotic stability are ensured by the use of a separable quadratic-type Lyapunov function, with a fixed-structure Lyapunov matrix, as well as the LaSalle's invariance principle. The effectiveness of the proposed voltage control strategy is evaluated through simulation case studies.

Keywords: DC microgrids, Voltage control, Lyapunov theory, LaSalle's invariance principle, PI control.

1. INTRODUCTION

Nowadays DC microgrids have drawn continually increasing attention due to their main advantages including higher efficiency, reduced losses, and easy and natural integration with renewable energy sources and energy storage resources (Dragicevic et al. (May 2016)). In the DC microgrid systems, the renewable energy sources with a DC-type output are normally interfaced to the microgrid through DC-DC power-electronic converters.

As the applicability of the DC microgrid systems is widely increasing, the design of appropriate control strategies which ensure microgrid's stability and efficiency plays an important role. One of the main challenges in DC microgrids with multiple distribution generation (DG) units is about the design of scalable voltage stabilization of DG units. In the scalable design, the main objective is that the stable operation of microgrids and the voltage control design are not influenced by uncertainty sources affected the architecture of the microgrid systems (Nasirian et al. (Dec. 2014)). The examples of the uncertainty sources are plug-and-play operation of DG units, structural/electrical upgrades, and faults/failure in the distribution lines connecting different DG units.

The most common control approaches for the DC microgrids are based on droop control (e.g. J. M. Guerrero et al. (Jan. 2011); Guerrero et al. (Apr. 2013); Meng et al. (Sept. 2017)) consisting of three control levels named as primary, secondary, and tertiary control. The primary control level aims to stabilize the voltage of DC microgrids and facilitate an accurate power sharing. The second level with slower time scale compensates for the deviations in the voltage in the steady state (Guerrero et al. (Apr. 2013)). The tertiary level assigns the microgrid voltage and is responsible for an optimal operation and power management in DC microgrids (Guerrero et al. (Apr. 2013); Nasirian et al. (Dec. 2014)). From a control point of view, the primary level has a decentralized proportional (P) control framework whereas the secondary level has centralized/distributed integral (I) control structure which relies on communication networks and information exchange among DG units' neighbors (Guerrero et al. (Apr. 2013)). In spite of the potential advantages of the droop-based control strategy, it comes at the expense of instability issues, slow dynamic responses, and dependency on the line impedance (Yazdanian and Mehrizi-Sani (Nov. 2014)).

Another category of voltage control strategies for DC microgrids is the so-called *non-droop-based* methods which combine primary and secondary control levels. Non-droop-based approaches are mainly based on decentralized advanced model-based control techniques (Sadabadi et al. (Nov. 2018)). Recently, several scalable voltage control approaches of DC microgrids have been proposed, e.g. Sadabadi et al. (Nov. 2018); Tucci et al. (Nov. 2016); M. Tucci et al. (May 2018); Sadabadi and Shafiee (Jan. 2020); Cucuzzella et al. (Jul. 2019); M. Cucuzzella et al. (Jul. 2019); Cucuzzella et al. (Mar. 2019). The proposed techniques which are mainly based on the Lyapunov theorem (e.g. Sadabadi et al. (Nov. 2018); Tucci et al. (Nov. 2016); M. Tucci et al. (May 2018)) and/or passivity theorem (e.g. Cucuzzella et al. (Jul. 2019); M. Cucuzzella et al. (Jul. 2019); Cucuzzella et al. (Mar. 2019)) provide a guarantee of voltage stability in the DC microgrids. However, they require information about the power lines connected to each distributed generation unit (Sadabadi et al. (Nov. 2018); Tucci et al. (Nov. 2016); Sadabadi and Shafiee (Jan. 2020); Cucuzzella et al. (Jul. 2019); M. Cucuzzella et al. (Jul. 2019); Cucuzzella et al. (Mar. 2019)). Furthermore, in these approaches, the proposed voltage control law, expressed in terms of a state-feedback control and/or some nonlinear control, requires solving optimization problems.

Considering the advantages and drawbacks of both droop-based and non-droop-based control strategies, we propose a voltage control framework which replaces the droop mechanism with a decentralized PI controller. The proposed control strategy enables us to take advantages of both droop-based and non-droop-based approaches. Similar to the droop control, the proposed approach is based on a PI control; however, it does not depend

on line parameters. Moreover, similar to the non-droop-base mechanism, the proposed method ensures the robust stability and reliable operation of DC microgrids. Explicit equalities on the proportional and integral terms of the stabilizing voltage controllers are provided. Therefore, the design procedure does not rely on a solution of optimization problems. Moreover, the local voltage control design is independent of the parameters of distribution lines. The proposed control stagey guarantees the asymptotic stability of the DC microgrid system. The scalability of the design and asymptotic stability are ensured by utilizing a Lyapunov-based framework with a separable quadratic-type structured Lyapunov function as well as LaSalle's invariance principle. The efficiency of the proposed voltage control strategy is evaluated via simulation case studies carried out in MATLAB/Simscape Electrical.

The rest of the paper is organized as follows. Section 2 presents a dynamical model of DC microgrids with DC-DC buck converters. The stabilizing PI voltage control framework and the proposed control design strategy are given in Section 3 and Section 4, respectively. Section 5 is devoted to simulation case studies. Section 6 concludes the paper.

The notation used in this paper is standard. In particular, matrix 0 is the zero matrix of appropriate dimensions. The symbols A^T and $A[i,j]$ denote the transpose of matrix A and the ij element of matrix A. For symmetric matrices, $P>0$ ($P<0$) and $P\geq 0$ ($P\leq 0$) respectively indicate the positive-definiteness (negative-definiteness) and the positive semi-definiteness (negative semi-definiteness).

2. DYNAMICAL MODEL OF DC MICROGRIDS

We consider an islanded DC microgrid with N DG units. The energy source of each DG is represented by a DC voltage source that supplies a local load through a DC-DC buck converter at the Point of Common Coupling (PCC). A schematic diagram of a buck-based DG is shown in Fig. 1. Different DG units are connected via distribution lines. DC microgrids are modeled as interconnected systems, where each DG forms a subsystem and the distribution lines represent the interactions among the subsystems. The symbols used in Fig. 1 are described in Table 1.

Graph Representation of DC Microgrids: The DC microgrid forms a network represented by a directed graph $\mathscr{G}=(\mathscr{V},\mathscr{E})$, where $\mathscr{V}$ and $\mathscr{E}$ are the sets of vertices and edges, respectively. Each element in the vertex set $\mathscr{V}=\{1,..,N\}$ represents a DG and each element in the edge set $\mathscr{E}=\{1,..,m\}$ represents the distribution line between the corresponding DG units. The microgrid topology is described by the incidence matrix $\mathscr{D}\in\mathbb{R}^{N\times m}$ of the directed graph $\mathscr{G}$. The incidence matrix $\mathscr{D}=[\mathscr{D}_{ik}]$ defines the direction of the distribution line current. If the current I_k leaves DG i and enters DG j, $\mathscr{D}_{ik}=1$ and $\mathscr{D}_{jk}=-1$ and if it enters the node i and leaves DG j, $\mathscr{D}_{ik}=-1$ and $\mathscr{D}_{jk}=1$. If the line k does not connect DG i and DG j, then $\mathscr{D}_{ik}=0$ and $\mathscr{D}_{jk}=0$. Therefore, $\mathscr{D}_{ik}$ is formulated as follows:

$$\mathscr{D}_{ik}=\begin{cases}1 & \text{if line } k \text{ leaves DG } i,\\ -1 & \text{if line } k \text{ enters DG } i,\\ 0 & \text{otherwise.}\end{cases} \tag{1}$$

for $i=1,\ldots,N$ and $k=1,\ldots,m$.

Model of a DG with a Buck Converter: Using Kirchhoff's current and voltage laws, each DG unit is mathematically modeled as follows:

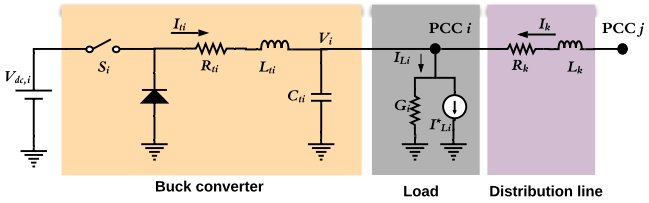

Fig. 1. A schematic diagram of a buck-based DG unit.

Table 1. Parameters of the DG Unit in Fig. 1.

(R_{t_i},L_{t_i})	Buck filter parameters
I_{t_i}	Filter current
C_{t_i}	Shunt capacitance
V_i	Voltage at PCC i
$V_{dc,i}$	Voltage of the input side of the DC-DC converter
G_i	Load conductance
$I^*_{L_i}$	Load constant current
I_{L_i}	Load current
(R_k,L_k)	Distribution lines parameters
I_k	Distribution lines current

$$\begin{aligned}\dot{x}_{g_i}&=A_{g_i}x_{g_i}+B_iu_i+B_{L_i}I_{L_i}+B_{l_i}\sum_{k\in\mathscr{E}_i}\mathscr{D}_{ik}I_k\\ y_i&=C_ix_{g_i}\end{aligned} \tag{2}$$

where $x_{g_i}=[\,V_i\ I_{t_i}\,]^T$ is the state, $u_i=V_{dc,i}d_i$ is the input, d_i is the duty cycle of the DC-DC converter, $y_i=V_i$ is the output, and I_{L_i} is the load current. The term $B_{l_i}\sum_{k\in\mathscr{E}_i}D_{ik}I_k$ describes the interaction between DG i and other DG units through the distribution lines k with current I_k, $k\in\mathscr{E}_i$. The set $\mathscr{E}_i\subset\mathscr{E}$ describes the set of the distribution lines connected to DG i. The state space matrices are given as follows:

$$\begin{aligned}A_{g_i}&=\begin{bmatrix}0 & \frac{1}{C_{t_i}}\\ -\frac{1}{L_{t_i}} & -\frac{R_{t_i}}{L_{t_i}}\end{bmatrix},\quad B_i=\begin{bmatrix}0\\ \frac{1}{L_{t_i}}\end{bmatrix}\\ B_{L_i}&=\begin{bmatrix}-\frac{1}{C_{t_i}}\\ 0\end{bmatrix},\quad B_{l_i}=\begin{bmatrix}-\frac{1}{C_{t_i}}\\ 0\end{bmatrix}\\ C_i&=[\,1\quad 0\,]\end{aligned} \tag{3}$$

Dynamics of Distribution Lines: It is assumed that there are m distribution lines in the DC microgrid system. The resistive-inductive distribution line k with parameters (R_k,L_k) and the line current I_k, from DG i to DG j, is modeled as follows:

$$\dot{I}_k=-\frac{R_k}{L_k}I_k+\frac{1}{L_k}(\mathscr{D}_{ik}V_i+\mathscr{D}_{jk}V_j) \tag{4}$$

Load Model: It is assumed that the loads are connected to the DG terminals at PCCs. The load current I_{L_i} in (2) is modeled as follows:

$$I_{L_i}=G_iV_i+I^*_{L_i} \tag{5}$$

where G_i is the load conductance and $I^*_{L_i}$ is a constant current load of DG i.

DC Microgrid Model: The overall microgrid system with the dynamics in (2) in presence of the loads in (5) can be presented as follows:

$$\begin{aligned}\dot{x}_{g_i}&=A_ix_{g_i}+B_iu_i+B_{L_i}I^*_{L_i}+B_{l_i}\sum_{k\in\mathscr{E}_i}\mathscr{D}_{ik}I_k\\ \dot{I}_k&=-\frac{R_k}{L_k}I_k+\frac{1}{L_k}\sum_{i=1}^{N}\mathscr{D}_{ik}V_i\\ y_i&=C_ix_{g_i}\end{aligned} \tag{6}$$

where

$$A_i = \begin{bmatrix} -\frac{G_i}{C_{t_i}} & \frac{1}{C_{t_i}} \\ -\frac{1}{L_{t_i}} & -\frac{R_{t_i}}{L_{t_i}} \end{bmatrix} \tag{7}$$

for $i = 1,\dots,N$ and $k = 1,\dots,m$.

3. PI-BASED VOLTAGE CONTROL FRAMEWORK

In this section, we formulate the control objectives aiming at the voltage stabilization of a DC microgrid system and voltage tracking by an appropriate design of PI controllers. The voltage controllers ensure that the voltage signals at PCCs track reference voltages $V_{ref,i}$ provided by a higher-level controller.

Control Structure: The control input of DG i, $i = 1,\dots,N$ can be structured as follows:

$$u_i = K_{P_i}(V_i - V_{ref,i}) + K_{I_i}\int(-V_i + V_{ref,i})dt \tag{8}$$

where K_{P_i} and K_{I_i} respectively are the proportional and the integral parameters of the PI controllers. The term $\int(-V_i + V_{ref,i})dt$ is defined as a new variable v_i with the following dynamics:

$$\dot{v}_i = -V_i + V_{ref,i} \tag{9}$$

Change of Coordinates: For a given $V_{ref,i}$ and $I^*_{L_i}$, the unique equilibrium point of (6)-(8) is given by:

$$\begin{aligned} \bar{V}_i &= V_{ref,i} \\ \bar{I}_k &= \frac{1}{R_k}\sum_{i=1}^{N}\mathscr{D}_{ik}V_{ref,i} \\ \bar{I}_{t_i} &= V_{ref,i}G_i + I^*_{L_i} + \sum_{k\in\mathscr{E}_i}\mathscr{D}_{ik}\bar{I}_k \\ \bar{u}_i &= V_{ref,i} + R_{t_i}\bar{I}_{t_i} \\ \bar{v}_i &= \frac{\bar{u}_i}{K_{I,i}}, \quad \bar{y}_i = V_{ref,i} \end{aligned} \tag{10}$$

By change of the coordinates as $\tilde{u}_i = u_i - \bar{u}_i$, $\tilde{y}_i = y_i - \bar{y}_i$, $\tilde{V}_i = V_i - \bar{V}_i$, $\tilde{I}_{t_i} = I_{t_i} - \bar{I}_{t_i}$, $\tilde{v}_i = v_i - \bar{v}_i$, and $\tilde{I}_k = I_k - \bar{I}_k$, the system dynamics in (6) and (9) can be rewritten as follows:

$$\begin{aligned} \dot{\tilde{x}}_i &= \tilde{A}_i\tilde{x}_i + \tilde{B}_i\tilde{u}_i + \tilde{B}_{l_i}\sum_{k\in\mathscr{E}_i}\mathscr{D}_{ik}\tilde{I}_k \\ \dot{\tilde{I}}_k &= -\frac{R_k}{L_k}\tilde{I}_k + \frac{1}{L_k}\sum_{i=1}^{N}\mathscr{D}_{ik}\tilde{V}_i \end{aligned} \tag{11}$$

where $\tilde{x}_i = \begin{bmatrix} \tilde{V}_i & \tilde{I}_{t_i} & \tilde{v}_i \end{bmatrix}^T$ and

$$\begin{aligned} \tilde{A}_i &= \begin{bmatrix} A_i & 0 \\ -C_i & 0 \end{bmatrix}, \quad \tilde{B}_i = \begin{bmatrix} B_i \\ 0 \end{bmatrix} \\ \tilde{B}_{l_i} &= \begin{bmatrix} B_{l_i} \\ 0 \end{bmatrix}, \quad \tilde{C}_i = [\,C_i \quad 0\,] \end{aligned} \tag{12}$$

Closed-loop System of DG i: The closed-loop system of DG i with the PI-based control law in (8) is presented as follows:

$$\begin{aligned} \dot{\tilde{x}}_i &= \tilde{A}_i\tilde{x}_i + \tilde{B}_i\tilde{u}_i + \tilde{B}_{l_i}\sum_{k\in\mathscr{E}_i}\mathscr{D}_{ik}\tilde{I}_k \\ \dot{\tilde{I}}_k &= -\frac{R_k}{L_k}\tilde{I}_k + \frac{1}{L_k}\sum_{i=1}^{N}\mathscr{D}_{ik}\tilde{V}_i \\ \tilde{u}_i &= K_{P_i}\tilde{V}_i + K_{I_i}\tilde{v}_i \\ \tilde{y}_i &= \tilde{C}_i\tilde{x}_i \end{aligned} \tag{13}$$

The main objective is to design the proportional and integral gains K_{P_i} and K_{I_i}, $i = 1,\dots,N$ which guarantee the stability of the DC microgrid system.

4. PROPOSED CONTROL DESIGN APPROACH

In this section, a solution for the PI-based voltage stabilization of the DC microgrid system, based on the Lyapunov theorem and the LaSalle's invariance principle (Khalil (2006)), is proposed.

4.1 VOLTAGE CONTROL DESIGN STRATEGY

Consider the following separable quadratic-type Lyapunov function for the microgrid system in (13) consisting of N DG units and m distribution lines:

$$\mathbf{V}(\tilde{\mathbf{x}},\tilde{I}) = \mathbf{V}_{line}(\tilde{I}) + \sum_{i=1}^{N}\mathbf{V}_i(\tilde{x}_i) \tag{14}$$

where $\tilde{\mathbf{x}} = \begin{bmatrix} \tilde{x}_1^T & \dots & \tilde{x}_N^T \end{bmatrix}^T$, $\tilde{I} = \begin{bmatrix} \tilde{I}_1 & \dots & \tilde{I}_m \end{bmatrix}^T$, and

$$\begin{aligned} \mathbf{V}_{line}(\tilde{I}) &= \sum_{k=1}^{m}\alpha L_k\tilde{I}_k^2 \\ \mathbf{V}_i(\tilde{x}_i) &= \tilde{x}_i^T P_i\tilde{x}_i \end{aligned} \tag{15}$$

where $\alpha > 0$ and $P_i > 0$ is a positive-definite matrix. The time derivative of $\mathbf{V}_{line}(\tilde{I})$ and $\mathbf{V}_i(\tilde{x}_i)$ along the closed-loop trajectories of (13) are as follows:

$$\dot{\mathbf{V}}_{line}(\tilde{I}) = -2\alpha\sum_{k=1}^{m}R_k\tilde{I}_k^2 + \alpha(\tilde{V}^T\mathscr{D}\tilde{I} + \tilde{I}^T\mathscr{D}^T\tilde{V}) \tag{16}$$

$$\begin{aligned} \dot{\mathbf{V}}_i(\tilde{x}_i) = {} & \tilde{x}_i^T(\tilde{A}_i^TP_i + P_i\tilde{A}_i)\tilde{x}_i + \tilde{x}_i^TP_i\tilde{B}_i\tilde{u}_i + \tilde{u}_i^T\tilde{B}_i^TP_i\tilde{x}_i \\ & + \sum_{k\in\mathscr{E}_i}\tilde{I}_k^T\mathscr{D}_{ik}\tilde{B}_{l_i}^TP_i\tilde{x}_i + \tilde{x}_i^TP_i\tilde{B}_{l_i}\sum_{k\in\mathscr{E}_i}\mathscr{D}_{ik}\tilde{I}_k \end{aligned} \tag{17}$$

where $\tilde{V} = \begin{bmatrix} \tilde{V}_1 & \dots & \tilde{V}_N \end{bmatrix}^T$.

By replacing $\tilde{u}_i$ with $\tilde{u}_i - \tilde{K}_i\tilde{x}_i + \tilde{K}_i\tilde{x}_i$, $\dot{\mathbf{V}}_i(\tilde{x}_i)$ is expressed as follows:

$$\begin{aligned} \dot{\mathbf{V}}_i(\tilde{x}_i) = {} & \tilde{x}_i^T\left((\tilde{A}_i + \tilde{B}_i\tilde{K}_i)^TP_i + P_i(\tilde{A}_i + \tilde{B}_i\tilde{K}_i)\right)\tilde{x}_i \\ & + (-\tilde{K}_i\tilde{x}_i + \tilde{u}_i)^T\tilde{B}_i^TP_i\tilde{x}_i + \tilde{x}_i^TP_i\tilde{B}_i(-\tilde{K}_i\tilde{x}_i + \tilde{u}_i) \\ & + \tilde{x}_i^TP_i\tilde{B}_{l_i}\sum_{k\in\mathscr{E}_i}\mathscr{D}_{ik}\tilde{I}_k + \sum_{k\in\mathscr{E}_i}\mathscr{D}_{ik}\tilde{I}_k^T\tilde{B}_{l_i}^TP_i\tilde{x}_i \end{aligned} \tag{18}$$

Therefore,

$$\begin{aligned} \dot{\mathbf{V}}(\tilde{\mathbf{x}},\tilde{I}) = {} & -2\alpha\sum_{k=1}^{m}R_k\tilde{I}_k^2 + \alpha(\tilde{V}^T\mathscr{D}\tilde{I} + \tilde{I}^T\mathscr{D}^T\tilde{V}) + \sum_{i=1}^{N}\tilde{x}_i^TQ_i\tilde{x}_i \\ & + \sum_{i=1}^{N}\left((-\tilde{K}_i\tilde{x}_i + \tilde{u}_i)^T\tilde{B}_i^TP_i\tilde{x}_i + \tilde{x}_i^TP_i\tilde{B}_i(-\tilde{K}_i\tilde{x}_i + \tilde{u}_i)\right) \\ & + \sum_{i=1}^{N}\left(\tilde{x}_i^TP_i\tilde{B}_{l_i}\sum_{k\in\mathscr{E}_i}\mathscr{D}_{ik}\tilde{I}_k + \sum_{k\in\mathscr{E}_i}\mathscr{D}_{ik}\tilde{I}_k^T\tilde{B}_{l_i}^TP_i\tilde{x}_i\right) \end{aligned} \tag{19}$$

where

$$Q_i = (\tilde{A}_i + \tilde{B}_i\tilde{K}_i)^TP_i + P_i(\tilde{A}_i + \tilde{B}_i\tilde{K}_i) \tag{20}$$

In the next theorem, we show that $\dot{\mathbf{V}}(\tilde{\mathbf{x}},\tilde{I}) \le 0$ for all $(\tilde{\mathbf{x}},\tilde{I})$ by an appropriate choice of $\tilde{u}_i$, $i = 1,\dots,N$.

Theorem 1. Consider the closed-loop microgrid system in (13). The following control law makes $\dot{\mathbf{V}}(\tilde{\mathbf{x}},\tilde{I}) \leq 0$ for all $(\tilde{\mathbf{x}},\tilde{I})$.

$$\tilde{u}_i = K_i \tilde{x}_i \tag{21}$$

where

$$K_i = \tilde{K}_i - \beta_i \tilde{B}_i^T P_i \tag{22}$$

where β_i is a real positive scalar and $P_i > 0$ has the following structure:

$$P_i = \alpha \begin{bmatrix} C_{t_i} & 0 & 0 \\ 0 & \rho_{2_i} & -\rho_{1_i}\rho_{2_i} \\ 0 & -\rho_{1_i}\rho_{2_i} & \rho_{1_i}(\rho_{1_i}\rho_{2_i}+1) \end{bmatrix} \tag{23}$$

and $\rho_{1_i} > 0$ and $0 < \rho_{2_i} < \alpha^{-1}\beta_i^{-1} R_{t_i} L_{t_i}$.

Moreover, the gain matrix $\tilde{K}_i = \begin{bmatrix} \tilde{k}_{1,i} & \tilde{k}_{2,i} & \tilde{k}_{3,i} \end{bmatrix}$ is obtained as follows:

$$\begin{aligned} \tilde{k}_{1,i} &= 1 - L_{t_i}(\rho_{2_i}^{-1} + \rho_{1_i}) \\ \tilde{k}_{2,i} &= \alpha\beta_i \frac{1}{L_{t_i}} \rho_{2_i} \\ \tilde{k}_{3,i} &= \rho_{1_i}(R_{t_i} - \tilde{k}_{2,i}) \end{aligned} \tag{24}$$

Proof 1. The proof of Theorem 1 is as follows:

Neutral interactions $\tilde{\mathbf{I}}_\mathbf{k}$. By employing P_i in (23), it can be shown that

$$\begin{aligned} \sum_{i=1}^{N} \left(\tilde{x}_i^T P_i \tilde{B}_{l_i} \sum_{k \in \mathscr{E}_i} \mathscr{D}_{ik} \tilde{I}_k + \sum_{k \in \mathscr{E}_i} \mathscr{D}_{ik} \tilde{I}_k^T \tilde{B}_{l_i}^T P_i \tilde{x}_i \right) \\ + \alpha(\tilde{V}^T \mathscr{D} \tilde{I} + \tilde{I}^T \mathscr{D}^T \tilde{V}) = 0 \end{aligned} \tag{25}$$

The above equation indicates that the interactions within the DC microgrid systems are neutral due to the structured Lyapunov matrix P_i in (23). As a result, (19) simplifies to:

$$\begin{aligned} \dot{\mathbf{V}}(\tilde{\mathbf{x}}) = -2\alpha \sum_{k=1}^{m} R_k \tilde{I}_k^2 + \sum_{i=1}^{N} \tilde{x}_i^T Q_i \tilde{x}_i \\ + \sum_{i=1}^{N} (-\tilde{K}_i \tilde{x}_i + \tilde{u}_i)^T \tilde{B}_i^T P_i \tilde{x}_i + \sum_{i=1}^{N} \tilde{x}_i^T P_i \tilde{B}_i (-\tilde{K}_i \tilde{x}_i + \tilde{u}_i) \end{aligned} \tag{26}$$

The first term in (26), i.e. $-2\alpha \sum_{k=1}^{m} R_k \tilde{I}_k^2$, is non-positive. In the next step, we show that $Q_i \leq 0$ for $i = 1, \ldots, N$.

$\mathbf{Q_i} \leq \mathbf{0}$. The negative semi-definiteness of Q_i is equivalent to the negative semi-definiteness of matrix $\tilde{Q}_i = P_i^{-1} Q_i P_i^{-1}$. We definite new matrices $Y_i = P_i^{-1}$ and $g_i = \tilde{K}_i P_i^{-1}$. As a result, $\tilde{Q}_i$ is presented as follows:

$$\tilde{Q}_i = Y_i \tilde{A}_i^T + \tilde{A}_i Y_i + \tilde{B}_i g_i + g_i^T \tilde{B}_i^T \tag{27}$$

Matrices $Y_i > 0$ and g_i are parametrized as follows:

$$Y_i = \begin{bmatrix} \alpha^{-1} C_{t_i}^{-1} & 0 & 0 \\ 0 & y_{22_i} & y_{23_i} \\ 0 & y_{23_i} & y_{33_i} \end{bmatrix} \tag{28}$$

$$\begin{aligned} g_i &= \begin{bmatrix} g_{1_i} & g_{2_i} & g_{3_i} \end{bmatrix} \\ &= \begin{bmatrix} \frac{\tilde{k}_{1,i}}{\alpha C_{t_i}} & \tilde{k}_{2,i} y_{22_i} + \tilde{k}_{3,i} y_{23_i} & \tilde{k}_{2,i} y_{23_i} + \tilde{k}_{3,i} y_{33_i} \end{bmatrix} \end{aligned} \tag{29}$$

By replacing Y_i and G_i in (27), $\tilde{Q}_i$ is rewritten as follows:

$$\tilde{Q}_i = \begin{bmatrix} -\frac{G_i}{C_{t_i}^2 \alpha} & \tilde{Q}_{12_i} & \tilde{Q}_{13_i} \\ \tilde{Q}_{12_i} & \tilde{Q}_{22_i} & \tilde{Q}_{23_i} \\ \tilde{Q}_{13_i} & \tilde{Q}_{23_i} & 0 \end{bmatrix} \tag{30}$$

where

$$\begin{aligned} \tilde{Q}_{12_i} &= \frac{1}{C_{t_i}} y_{22_i} - \frac{1}{\alpha C_{t_i} L_{t_i}} + \frac{1}{L_{t_i}} g_{1_i} \\ \tilde{Q}_{13_i} &= \frac{1}{C_{t_i}} y_{23_i} - \frac{1}{\alpha C_{t_i}} \\ \tilde{Q}_{22_i} &= -2\frac{R_{t_i}}{L_{t_i}} y_{22_i} + 2\frac{1}{L_{t_i}} g_{2_i} \\ \tilde{Q}_{23_i} &= -\frac{R_{t_i}}{L_{t_i}} y_{23_i} + \frac{1}{L_{t_i}} g_{3_i} \end{aligned} \tag{31}$$

The non-positiveness of $\tilde{Q}_i \leq 0$ implies that the third column and row of $\tilde{Q}_i$ must be equal to zero. We also consider $\tilde{Q}_{12_i} = 0$. As a result,

$$\begin{aligned} y_{23_i} &= \frac{1}{\alpha} \\ g_{3_i} &= \frac{R_{t_i}}{\alpha} \\ y_{33_i} &= \frac{1}{\alpha k_{3,i}} (R_{t_i} - \tilde{k}_{2,i}) \\ y_{22_i} &= \frac{1}{\alpha L_{t_i}} (1 - \tilde{k}_{1,i}) \end{aligned} \tag{32}$$

By replacing y_{23_i}, y_{22_i}, y_{33_i}, and g_{3_i} from (32) and g_{2_i} from (29) in (31), it can be shown that $\tilde{Q}_{22_i}$ simplifies as follows:

$$\tilde{Q}_{22_i} = \frac{2}{L_{t_i}} \tilde{k}_{3,i} (-\alpha y_{33_i} y_{22_i} + \frac{1}{\alpha}) \tag{33}$$

As $Y_i = P_i^{-1}$, it can be easily shown that $-\alpha y_{33_i} y_{22_i} + \frac{1}{\alpha} = -\alpha y_{33_i} \rho_{2_i}^{-1}$ where $\rho_{2_i} = P_i[2,2]$. Due to the positive definiteness of P_i, ρ_{2_i} is a positive scalar. Therefore, Y_i and $\tilde{Q}_i$ are presented as follows:

$$\begin{aligned} Y_i &= \begin{bmatrix} \alpha^{-1} C_{t_i}^{-1} & 0 & 0 \\ 0 & \alpha^{-2} y_{33_i}^{-1} + \rho_{2_i}^{-1} & \alpha^{-1} \\ 0 & \alpha^{-1} & y_{33_i} \end{bmatrix} \\ \tilde{Q}_i &= \begin{bmatrix} -\frac{G_i}{C_{t_i}^2 \alpha} & 0 & 0 \\ 0 & -\frac{2\alpha}{L_{t_i}} \tilde{k}_{3,i} y_{33_i} \rho_{2_i}^{-1} & 0 \\ 0 & 0 & 0 \end{bmatrix} \end{aligned} \tag{34}$$

If we assume that $\tilde{k}_{3,i} > 0$, $\tilde{Q}_i \leq 0$; therefore, $Q_i \leq 0$.

PI control law $\mathbf{u_i}$. We consider the control law as $\tilde{u}_i = \tilde{K}_i \tilde{x}_i - \beta_i \tilde{B}_i^T P_i \tilde{x}_i$ with a real positive scalar β_i. Therefore, $\dot{\mathbf{V}}(\tilde{\mathbf{x}})$ is expressed as follows:

$$\dot{\mathbf{V}}(\tilde{\mathbf{x}},\tilde{I}) = -2\alpha \sum_{k=1}^{m} R_k \tilde{I}_k^2 + \sum_{i=1}^{N} \tilde{x}_i^T Q_i \tilde{x}_i - 2\sum_{i=1}^{N} \beta_i \tilde{x}_i^T P_i \tilde{B}_i \tilde{B}_i^T P_i \tilde{x}_i \tag{35}$$

Since $-\beta_i \tilde{x}_i^T P_i \tilde{B}_i \tilde{B}_i^T P_i \tilde{x}_i \leq 0$, $\dot{\mathbf{V}}(\tilde{\mathbf{x}},\tilde{I}) \leq 0$ for all $(\tilde{\mathbf{x}},\tilde{I})$. Due to the structure of $\tilde{u}_i = K_{P_i} \tilde{V}_i + K_{I_i} \tilde{v}_i$, the term $(\tilde{k}_{i,2} - \frac{\beta_i}{L_{t_i}} \rho_{2_i}) \tilde{I}_{t_i}$ must be equal to zero. Therefore, there is the following equality constraint on $\tilde{k}_{2,i}$ and ρ_{2_i}:

$$\tilde{k}_{2,i} = \frac{\beta_i}{L_{t_i}} \rho_{2_i} \tag{36}$$

Constraints on $\tilde{\mathbf{K}}_\mathbf{i}$. From (32), (33), and (36), the gain matrix $\tilde{K}_i$ is subject to the following constraints:

$$\begin{aligned} &y_{22_i} > 0 \Rightarrow \tilde{k}_{1,i} < 1 \\ &y_{33_i} > 0 \Rightarrow \tilde{k}_{2,i} < R_{t_i} \\ &\tilde{k}_{2,i} = \frac{\beta_i}{L_{t_i}} \rho_{2i} \\ &\tilde{Q}_{22_i} \leq 0 \Rightarrow \tilde{k}_{3,i} > 0 \end{aligned} \tag{37}$$

Structure of the Lyapunov matrix $\mathbf{P_i}$. Since $P_i = Y_i^{-1}$, the matrix P_i is structured as (23), where $\rho_{1_i} = \frac{1}{\alpha y_{33_i}} > 0$ and $\rho_{2_i} > 0$. Moreover, based on (36) and the inequality constraint on $\tilde{k}_{2,i}$ in (37), the choice of ρ_{2_i} must satisfy the following constraint:

$$0 < \rho_{2_i} < \alpha^{-1} \beta_i^{-1} R_{t_i} L_{t_i} \tag{38}$$

Explicit equalities on gain matrix $\tilde{\mathbf{K}}_\mathbf{i}$. From (32), (36), and the relationship between Y_i and P_i, the gain matrix $\tilde{K}_i$ is obtained as (24).

Proportional and integral gains $(\mathbf{K_{P_i}}, \mathbf{K_{I_i}})$. The proportional and integral terms of the PI controllers are obtained as follows:

$$\begin{aligned} K_{P_i} &= \tilde{k}_{i,1} = 1 - L_{t_i}(\rho_{2_i}^{-1} + \rho_{1_i}) \\ K_{I_i} &= \tilde{k}_{i,3} + \frac{\alpha \beta_i}{L_{t_i}} \rho_{1_i} \rho_{2_i} \\ &= \rho_{1_i} R_{t_i} \end{aligned} \tag{39}$$

for $i = 1, \ldots, N$.

Theorem 2. The PI control law given in (21) and (22) with the coefficients in (39) guarantees the stability of the closed-loop microgrid system.

Proof 2. In Theorem 1, it is shown that $\dot{\mathbf{V}}(\tilde{\mathbf{x}}, \tilde{I}) \leq 0$ for all $(\tilde{\mathbf{x}}, \tilde{I})$. We use the LaSalle's invariance principle to show that the closed-loop microgrid system with control law given in (21) is asymptotically stable. To this end, we need to show that the only solution of $\dot{\mathbf{V}}(\tilde{\mathbf{x}}, \tilde{I}) = 0$ is $(\tilde{\mathbf{x}}, \tilde{I}) = 0,\ \forall t > 0$. To see this, note that $\dot{\mathbf{V}}(\tilde{\mathbf{x}}, \tilde{I}) = 0$ implies that

$$\begin{aligned} \tilde{I}_k &= 0 \\ \tilde{x}_i^T Q_i \tilde{x}_i &= 0 \\ \tilde{B}_i^T P_i \tilde{x}_i &= 0 \end{aligned} \tag{40}$$

for $k = 1, \ldots, m$ and $i = 1 \ldots, N$. It is required to show that the only state trajectory of the system which satisfies all the constraints in (40) is origin. Let's compute the set χ as follows:

$$\chi = \underbrace{\{\tilde{I}_k = 0\}}_{\chi_1} \cap \underbrace{\{\tilde{x}_i : \tilde{x}_i^T Q_i \tilde{x}_i = 0\}}_{\chi_2} \cap \underbrace{\{\tilde{x}_i : \tilde{x}_i^T P_i \tilde{B}_i \tilde{B}_i^T P_i \tilde{x}_i = 0\}}_{\chi_3} \tag{41}$$

From the set χ_1, it is concluded that

$$\tilde{I}_k = 0 \Rightarrow \dot{\tilde{I}}_k = 0 \Rightarrow \tilde{V}_i = \tilde{V}_j; \quad i, j \in \mathscr{V} \tag{42}$$

Based on the set χ_2, we should find a state trajectory $\tilde{x}_i^\star$ which maximizes the term $f(\tilde{x}_i) = \tilde{x}_i^T Q_i \tilde{x}_i$. Note that the maximum value of $f(\tilde{x}_i)$ is zero. Therefore,

$$\left. \frac{df(\tilde{x}_i)}{d\tilde{x}_i} \right|_{\tilde{x}_i^\star} = 2 Q_i \tilde{x}_i^\star = 0 \tag{43}$$

By premultiplying of the above equation by $Y_i = P_i^{-1}$ and defining a new variable $\tilde{y}_i^\star = Y_i^{-1} \tilde{x}_i^\star$, we have

$$\tilde{Q}_i \tilde{y}_i^\star = 0 \tag{44}$$

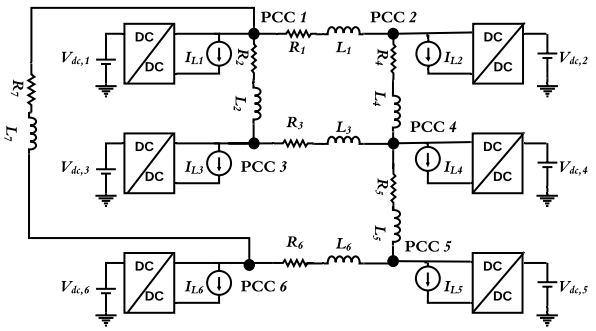

Fig. 2. Layout of an islanded DC microgrid with 6 DG units and 7 distribution lines.

where $\tilde{Q}_i$ and Y_i are defined in (34). It can be shown that the vector $\tilde{y}_i^\star$ satisfying (44) is characterized as $\tilde{y}_i^\star = \begin{bmatrix} 0 & 0 & \tilde{y}_{3,i}^\star \end{bmatrix}^T$. As a result, we have

$$\begin{aligned} \tilde{x}_i^\star &= Y_i \tilde{y}_i^\star \\ &= \begin{bmatrix} 0 & \frac{1}{\alpha} \tilde{y}_{3,i}^\star & \tilde{y}_{3,i}^\star y_{33_i} \end{bmatrix}^T \end{aligned} \tag{45}$$

Therefore, the state trajectory which satisfies the conditions in set χ_2 is in the form of (45). As a result,

$$\tilde{V}_i = 0 \Rightarrow \dot{\tilde{V}}_i = 0 \xRightarrow{\tilde{I}_k = 0} \tilde{I}_i = 0 \tag{46}$$

Moreover,

$$\tilde{I}_i = 0 \Rightarrow \tilde{y}_{3,i}^\star = 0 \xRightarrow{\tilde{v}_i = \tilde{y}_{3,i}^\star y_{33_i}} \tilde{v}_i = 0 \tag{47}$$

From (42), (46), and (47), we have

$$\chi_1 \cap \chi_2 = \{\tilde{x}_i = 0 \quad \& \quad \tilde{I}_k = 0\} \tag{48}$$

Since $\{\tilde{x}_i = 0\} \in \chi_3$, the largest invariant set of χ is origin, and therefore there are not any other state trajectories that converge to the origin. As a result, the origin in (13) is asymptotically stable.

4.2 PROPOSED VOLTAGE CONTROL DESIGN ALGORITHM

The PI voltage controller design for each DG whose dynamics are given in (13) is based on the following steps.

Input: Model of each DG.

Output: Decentralized PI voltage controllers K_i.

(i) Design of the structured Lyapunov matrix P_i in (23) by choosing ρ_{1_i} and ρ_{2_i}.
(ii) Finding the coefficients of the PI controllers in (39).

5. SIMULATION RESULTS

In order to evaluate the proposed voltage control scheme, simulation studies are performed on an islanded DC microgrid with DC-DC buck converters, borrowed from Sadabadi et al. (Nov. 2018). The microgrid consists of $N = 6$ DG units and $m = 7$ distribution lines as graphically shown in Fig. 2. The parameters of each DG and the distribution lines are given in Sadabadi et al. (Nov. 2018).

The stabilizing PI voltage controller of each DG is designed by using the proposed algorithm in Subsection 4.2. The voltage controllers are applied to the DC microgrid in Fig. 2 implemented in MATLAB/Simscape Electrical.

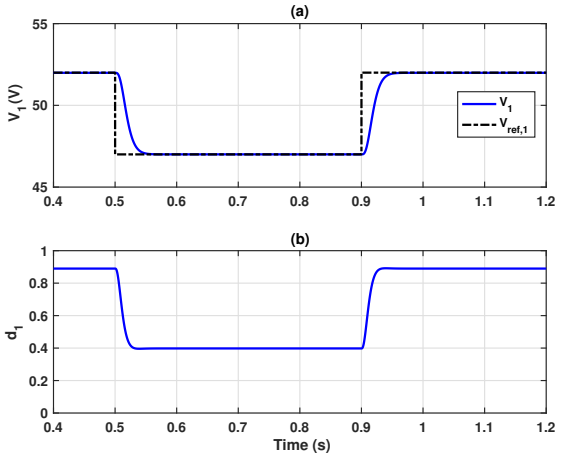

Fig. 3. Dynamic response of DG1 due to voltage reference changes: (a) voltage signal at PCC1 and (b) duty cycle of the buck converter of DG1.

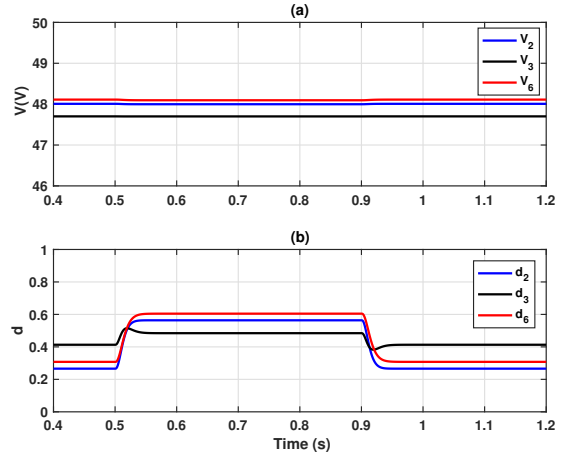

Fig. 4. Dynamic response of the neighbors of DG1 due to voltage reference changes at PCC1: (a) voltage signal at PCC2, PCC3, and PCC6 and (b) duty cycle of the buck converter of DG2, DG3, and DG6.

The performance and transient behavior of DG1 in voltage tracking scenario is assessed in this study. The voltage reference of DG1 is initially set at $52V$. Then, the reference is stepped down to $47V$ at $t = 0.5s$ and stepped up to $52V$ at $t = 0.9s$. Fig. 3 shows the dynamic responses of DG1. The results indicate that the proposed voltage control technique is able to regulate the voltage at PCCs with zero steady state error and small transient time.

The voltage signals at PCC2, PCC3, and PCC6 as well as the control inputs of DG2, DG3, and DG6 are depicted in Fig. 4. As one can observe from Fig. 4, due to the line-independent voltage control design, the voltage changes at PCC1 have negligible effects on the voltage signals of the neighbors of DG1.

6. CONCLUSION

This paper studies the scalable voltage stabilization for DC microgrids with DC-DC buck converters. Using a Lyapunov-based framework together with the LaSalle's invariance principle, a decentralized PI-based voltage controller is proposed, which relies on only the local electrical parameters of each DG unit. A set of parameters of stabilizing PI-based voltage controllers is presented. The control design strategy is scalable and allows the plug-and-play operation of DG units. The proposed voltage control scheme guarantees the asymptotic stability of the DC microgrid systems. Future works include the extension of our results to boost converters and DC microgrids with constant power loads.

REFERENCES

Cucuzzella, M., Kosaraju, K.C., and Scherpen, J.M.A. (Jul. 2019). Distributed passivity-based control of DC microgrids. In *American Control Conference (ACC)*, 652–657. Philadelphia, PA, USA.

Cucuzzella, M., Lazzari, R., Kawano, Y., Kosaraju, K.C., and Scherpen, J.M.A. (Mar. 2019). Robust passivity-based control of boost converters in DC microgrids. URL `https://arxiv.org/abs/1902.10273`.

Dragicevic, T., Lu, X., Vasquez, J.C., and Guerrero, J.M. (May 2016). DC microgrids– Part II: A review of power architectures, applications, and standardization issues. *IEEE Trans. Power Electron.*, 31(5), 3528–3549.

Guerrero, J.M., Chandorkar, M., Lee, T., and Loh, P.C. (Apr. 2013). Advanced control architectures for intelligent microgrids–Part I: Decentralized and hierarchical control. *IEEE Trans. Ind. Electron.*, 60(4), 1254–1262.

J. M. Guerrero, J. C. Vasquez, J. Matas, L. G. de Vicuna, and M. Castilla (Jan. 2011). Hierarchical control of droop-controlled AC and DC microgrids–A general approach towards standardization. *IEEE Trans. Ind. Electron.*, 58(1), 158–172.

Khalil, H.K. (2006). *Nonlinear Systems*. Prentice Hall, New Jersey.

M. Cucuzzella, K. C. Kosaraju, and J. M. A. Scherpen (Jul. 2019). Voltage control of DC networks: Robustness for unknown ZIP-loads. URL `https://arxiv.org/abs/1907.09973`.

M. Tucci, S. Riverso, and G. Ferrari-Trecate (May 2018). Line-independent plug-and-play controllers for voltage stabilization in DC microgrids. *IEEE Trans. Control Syst. Technol.*, 26(3), 1115–1123.

Meng, L., Shafiee, Q., Trecate, G.F., Karimi, H., Fulwani, D., and Lu, X. (Sept. 2017). Review on control of dc microgrids and multiple microgrid clusters. *IEEE Journal of Emerging and Selected Topics in Power Electronics*, 5(3), 928–948.

Nasirian, V., Davoudi, A., Lewis, F.L., and Guerrero, J.M. (Dec. 2014). Distributed adaptive droop control for DC distribution systems. *IEEE Trans. Energy Convers.*, 29(4), 944–956.

Sadabadi, M.S. and Shafiee, Q. (Jan. 2020). Robust voltage control of DC microgrids with uncertain constant power loads. *IEEE Trans. Power Systems*, 35(1), 508–515.

Sadabadi, M.S., Shafiee, Q., and Karimi, A. (Nov. 2018). Plug-and-play robust voltage control of DC microgrids. *IEEE Trans. Smart Grid*, 9(6), 6886–6896.

Tucci, M., Riverso, S., Vasquez, J.C., Guerrero, J.M., and Ferrari-Trecate, G. (Nov. 2016). A decentralized scalable approach to voltage control of DC islanded microgrids. *IEEE Trans. Control Syst. Technol.*, 24(6), 1965–1979.

Yazdanian, M. and Mehrizi-Sani, A. (Nov. 2014). Distributed control techniques in microgrids. *IEEE Trans. Smart Grid*, 5(6), 2901–2909.